

Received April 3, 2019, accepted May 6, 2019, date of publication May 20, 2019, date of current version June 17, 2019.

Digital Object Identifier 10.1109/ACCESS.2019.2917791

Autonomous Underwater Vehicle Vision Guided Docking Experiments Based on L-Shaped Light Array

ZHEPING YAN, PENG GONG^{ID}, WEI ZHANG, ZIXUAN LI, AND YANBIN TENG^{ID}

College of Automation, Harbin Engineering University, Harbin 150001, China

Corresponding author: Wei Zhang (dawizw@163.com)

This work was supported in part by the National Natural Science Foundation of China under Grant 51309067, in part by the Natural Science Foundation of Heilongjiang Province of China under Grant E2016020, and in part by the Fundamental Research Funds for the Central Universities under Grant HEUCFP201736 and Grant HEUCFM171011.

ABSTRACT In order to realize recovery of an autonomous underwater vehicle (AUV), the L-shaped light array installed at the bottom of the fork-carrying-pole docking device is designed, and the visual positioning algorithm based on the L-shaped light array is proposed. The L-shaped light array is identified by a camera installed on the abdomen of the AUV, the relative position deviation from the AUV and the light array is calculated, and the AUV is docked according to the obtained positional deviation. The monocular four-degree-of-freedom positioning algorithm for AUV solves the problem of missing part of the target light source. Judging the heading angle is improved when the AUV has a longitudinal inclination (heeling angle). The docking experiment of AUV recovery is carried out to verify the feasibility of the L-shaped light array as visual guidance and the stability of the positioning algorithm.

INDEX TERMS Autonomous underwater vehicle, L-shaped light array, vision guidance, positioning algorithm.

I. INTRODUCTION

AUV has endurance and extensive applications for marine research, ecological monitoring and other fields [1], [2]. Due to the limitation of volume and quality, the energy carried by AUV is very limited [3]. For AUV operating in a long time, the AUV must be distributed and recycled through the support platform to supplement energy, transfer information and maintain security [4]. It is impossible to ensure the concealment of the recovery platform by using the surface ship for deployment and recovery, and it is vulnerable to the interference from surface waves and cannot recover AUV under complex sea conditions [5]. Therefore, setting up a recovery dock into water to realize autonomous recovery of AUV has become a significant research direction [6].

In the aspect of underwater recovery system design, scientists at home and abroad have designed a variety of underwater recovery docking systems according to the characteristics of AUV and the types of recovery docking stations [7]–[14]. The docking method that takes ropes and rods as docking

targets [7], [8], such as an underwater capture docking system proposed by American scholars for Odyssey II UUV [7], which can dock in all directions, is less affected by the surrounding environment. And the reliability of docking is higher, but the structure of docking base station is more complicated. At the same time, the AUV is greatly changed; The docking method that takes the guide cover or cage as the docking target [9]–[13], such as REMUS UUV underwater docking system developed by Woods Hole Oceanographic Research Institute in the United States [9]. The docking device itself is not particularly complex, and there is not requirement for special modification of UUV. It has a protective effect after UUV docking, but it is more susceptible to the influence of current; the docking method that takes the platform as the docking target, such as Japan's Marine-bird underwater docking system [14]. The docking mode has a high probability of success. However, there are higher requirements for the power system and the self-guidance system of the underwater vehicle.

The automatic docking of AUV based on visual detection sensor is a complicated task in the aspect of AUV close-range

The associate editor coordinating the review of this manuscript and approving it for publication was Haiyong Zheng.

guidance and recovery docking [15]–[17]. Scholars from various countries have proposed a variety of docking methods based on visual sensors: detecting colors, self-similar signposts [18], identifying 3D shapes and guiding light arrays [19], etc. Aiming at the problem of detection target selection, GhoshS and others have verified that it is more suitable for underwater environment to use guidance light array as the target to be detected. The design of guiding light array includes linear light array composed of multiple lights [20], circular light array composed of multiple lights [21], square light array composed of four lights [12], etc. Linear light arrays are arranged in a straight line by multiple target lights, and the central light target is a special shape. The linear light array is applied to the platform type docking station. The structure of the linear light array is simple and easy to maintain. However, the light array cannot provide AUV with the direction of docking information, and the matching positioning algorithm will fail when the central light source is obscured. The circular light array and the square light array composed of multiple lights can calculate four-degree-of-freedom information, but only applicable to the guide cover as the target of the docking mode, in the case of some light source is obscured, there is a great potential to lead to docking failure.

In the following, part 2 introduces the design of L-shaped light array and the algorithm for judging the target light source. In part 3, based on the L-shaped light array, a monocular four-degree-of-freedom positioning algorithm of AUV is designed, which solves the problem of the location of some target light source loss. Moreover, the problem of judging the heading angle under the condition that the AUV has a longitudinal inclination angle (transverse inclination angle) is improved to realize accurate control of the heading of the AUV. In part 4, AUV recovery docking experiment is conducted to the feasibility of the recovery docking device and the stability of the visual positioning algorithm proposed in part 3. Finally, part 5 presents the conclusion.

II. FORK-CARRYING-POLE DOCKING DEVICE

A. COMPOSITION OF THE FORK-CARRYING-POLE DOCKING DEVICE

The AUV used to test is a small AUV independently designed by the laboratory team. The AUV could achieve lateral, longitudinal, vertical movement and change direction. In order to realize the recovery method of this paper, a slight modification is required to the AUV. A docking rod with a length of 0.5 m is installed in front of the camera in the belly of the AUV, as shown in Figure 1.

The fork-carrying-pole recovery device could realize autonomous recovery of AUV. The recovery device consists of four parts: the main structure, the V-shaped shears, the locking device and the L-shaped light array shown in Figure 2.

The main structure is a support structure, in which an acoustic beacon is fixed in it. The acoustic beacon and the

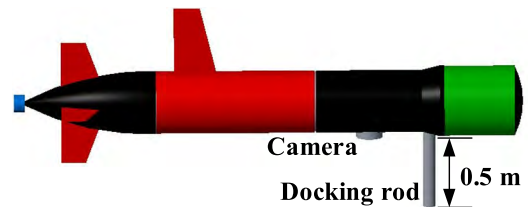


FIGURE 1. Schematic diagram of modified AUV.

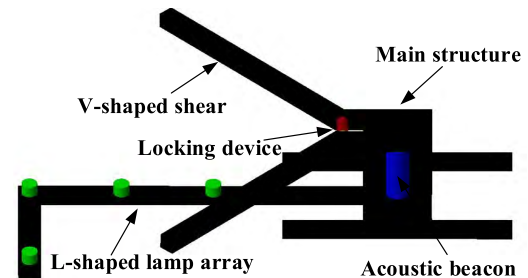


FIGURE 2. Schematic diagram of recovery device.

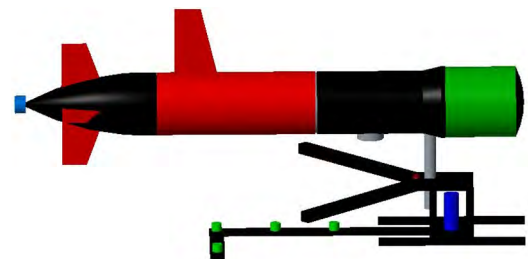


FIGURE 3. Schematic diagram of successful docking.

ultra-short baseline array mounted on the AUV head form the acoustic navigation system. The V-shaped shears are installed above the main structure. Two arms of the V-shaped shears have an open angle of 90° . The length of the arm is 100 cm, which provide guidance for the AUV docking rod. The locking device is arranged at the tail end of the V-shaped shears. When the docking rod of the AUV is captured by the V-shaped shears, the locking device locks the docking rod. The L-shaped light array is installed below the V-shaped shears to provide visual guidance. Figure 3 is a schematic diagram of successful docking.

B. DESIGN OF L-SHAPED LIGHT ARRAY

A kind of L-shaped light array which can realize AUV visual guidance is designed on the premise of AUV fork-carrying-pole recovery method. By identifying the light source target for the L-shaped light array, the vertical, longitudinal, transverse deviation and heading angle deviation of the AUV relative to the recovery device are calculated. The AUV is controlled to dock according to the obtained position deviation. In the process of fork-carrying-pole recovery, the precision of AUV heading angle deviation is higher, and the accuracy requirement can be met by using L-shaped light array.

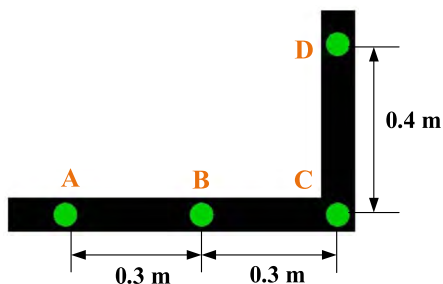


FIGURE 4. Schematic diagram of L-shaped light array.

As Figure 4 shows, the L-shaped light array is installed at the bottom of the recovery device and consists of 4 target light sources. There are three light sources in the longitudinal direction, and the spacing of each light target is 0.3 m, which are respectively marked as A, B and C; A light source is arranged along the transverse direction of 0.4 m with C as the center, denoted as D. So, the total longitudinal length of the L-shaped light array is 0.6 m and the total transverse length is 0.4 m. The target light sources of the L-shaped light array all adopt the same type of LED flashlights to ensure the same shape and luminous area.

The illumination intensity of target light sources gradually decreases of the increase in underwater illumination distance. The number of target light sources can be increased to improve the visual guidance range to some extent. There is no specific requirement for the number of target light sources, as long as the target light source is arranged in L-shaped order. The four target light sources represent the key positions of the L-shaped light array. In actual AUV recovery, the number of target light sources may not be limited to four.

C. EXTRACTION AND DISCRIMINATION OF TARGET LIGHT SOURCE

In order to obtain the target light source, a series of image preprocessing is needed for the captured image. Firstly, the image is filtered by mean filter to eliminate the Gaussian noise commonly used in underwater images. Secondly, the image obtained in the previous step is quickly segmented by region growing method, and the target light source region is extracted. GVF Snake algorithm is used to identify and smooth the contour. Finally, the processed gray-scale image is binarized to become a binary image. Figure 5 shows the processed image. The contour of the image target area is obvious, the boundary is smooth and does not contain noise.

The image captured by the camera not only contains noise, but also may contain bubbles and reflective substances in the pool. The causes interference to the real light source target recognition. Although the previous preprocessing of the image eliminates the vast majority of noise, the pseudo-light source formed by bubbles and reflective substances still exists. The Blob analysis method is introduced to describe the morphological characteristics of real light sources, such as roundness, roughness, tightness, solid degree, convexity, etc. Based on Blob analysis method, geometric constraints

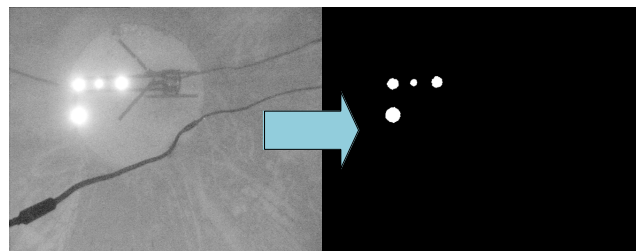


FIGURE 5. Images before and after preprocessing.

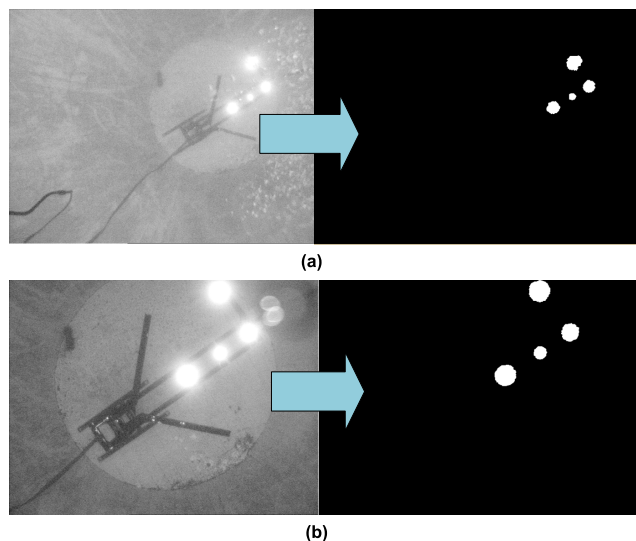


FIGURE 6. Images before and after removal bubbles (a) and images before and after removal reflective substances (b).

and area constraints are generated. The Bayesian minimum error rate is used to eliminate pseudo-light sources to obtain real light source targets. The original image and the removal result are shown in the Figure 6.

After obtaining real light source targets, extract their central coordinates in the image, and judge the relative positions of the four target light sources. That is, determine the relative position of light A, light B, light C and light D in the L-shaped light array.

The algorithm for judging the relative position of the target light sources is as follows:

- (1) Define the center coordinates of the four light source targets in turn as A, B, C, D. Take any two points to generate a straight line. That is, $l_{AB}, l_{BC}, l_{AC}, l_{AD}, l_{BD}, l_{CD}$.
- (2) Calculate the included angle between any two straight lines Δ . Select a straight line to make $\Delta \leq 5^\circ$. l_{AB}, l_{BC}, l_{AC} are almost collinear, the three lines are selected. Three candidate points of light A, light B and light C can be selected.
- (3) Determine the target light source for the light D. Light D can be judged by (2) what the number of known target light sources is four, and the remaining target light source is the light D.
- (4) Calculate the distances ρ between light D and the other three points. Select the maximum distance line segment, and the both sides of the line segment are point A and D. Select the minimum distance line segment, and the both sides of

TABLE 1. Target light source A, B, C, D discriminating results.

Simulation image	Target light source pixel position	
	A	[533.262, 182.583]
	B	[525.452, 128.156]
	C	[516.865, 79.2127]
	D	[445.443, 86.0985]
	A	[481.102, 220.902]
	B	[518.906, 181.335]
	C	[550.945, 146.921]
	D	[499.954, 98.0526]
	A	[255.526, 182.862]
	B	[201.048, 181.811]
	C	[151.523, 182.805]
	D	[149.088, 254.664]
	A	[262.009, 182.745]
	B	[210.542, 165.301]
	C	[163.843, 150.751]
	D	[139.803, 217.731]

the line segment are point C and D. The rest of the point is light B.

Four AUV images taken at any position are simulated, and the simulation results are shown in Table 1. The L-shaped light array appearing anywhere in the image can calculate the pixel coordinates of these target light sources and identify the target light source A, B, C, D, thus the correctness and rationality of the target light source judging algorithm are verified.

III. VISUAL GUIDANCE FOR FORK-CARRYING-POLE DOCKING

A. ESTABLISHMENT OF DOCKING COORDINATE SYSTEM

Establish docking system coordinate systems, including: AUV docking rod coordinate system $O^aX^aY^aZ^a$, Camera coordinate system $O^cX^cY^cZ^c$, Image coordinate system O^uV , Image plane coordinate system OXY and L-shaped light array coordinate system $O^lX^lY^lZ^l$, as shown in Figure 7.

B. VISUAL GUIDANCE STRATEGY AND PROCESS

According to the structural characteristics of the fork-carrying-pole recovery device, a recovery strategy of “positioning-to-L-shaped” is designed. The core of the recovery strategy is to determine the three degrees of freedom of the AUV in the transverse direction, the longitudinal direction and the vertical direction and the heading angle deviation from the long side ‘|’ of the “L”, the short side ‘-’ of the “L” determines the heading of AUV. There are two target light source points A and C on the longitudinal central line of the recovery device, their center B is the center of the light array.

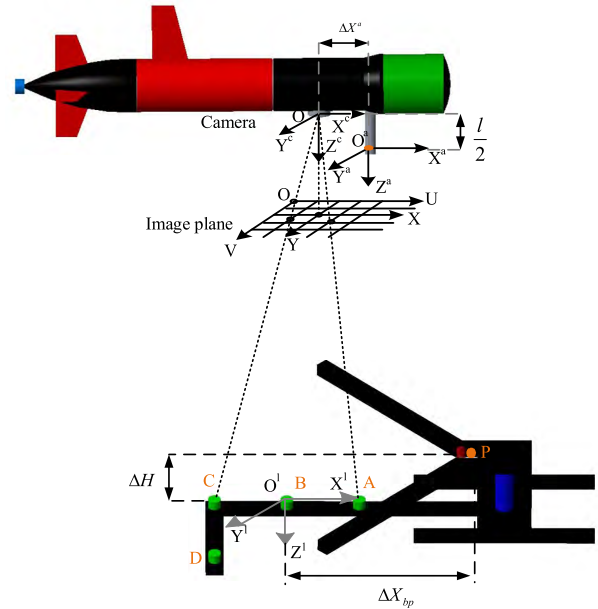


FIGURE 7. Establishment of coordinate system.

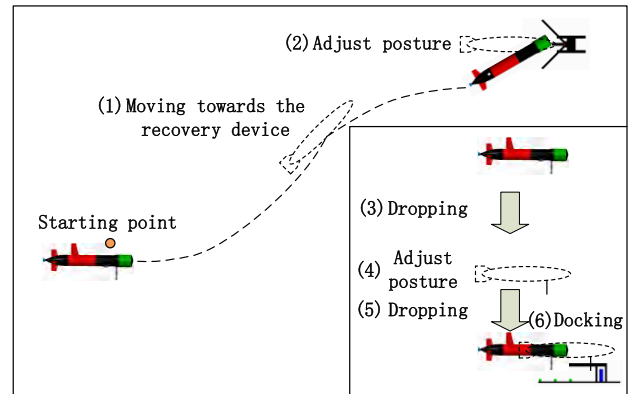


FIGURE 8. AUV fork-carrying-pole recovery flow chart.

The light D is vertically added on one side of the light C. The distance between A and C is not equal to the distance between C and D.

Firstly, AUV obtains and discriminates the relative positions of four target light sources through the target recognition algorithm designed in this paper. Since the locking device is close to one end of the light A and the short side ‘-’ of the “L” formed by light C and light D is located at the other end, it can be determined that \vec{CA} is the positive direction toward the AUV. The AUV adjusts the heading angle and controls its own movement so that it is parallel to and close to \vec{CA} . \vec{CA} is the long side ‘|’ of the “L” formed by light A and light C in a horizontal plane. The AUV keeps the above posture and moves towards the recovery device.

The AUV fork-carrying-pole recycling process, shown in Figure 8, can be divided into six phases:

(1) Start the acoustic guidance system to remotely locate the AUV and guide the AUV from the starting point to the recovery site.

(2) The AUV reaches effective visual guidance range by using the acoustic guidance system. Turn on the visual guidance system. According to the transverse, longitudinal and heading angle deviations measured by the visual guidance system, the AUV's position relative to the recovery device is adjusted in the horizontal plane.

(3) The AUV moves downward until it is 2 m above the recovery device according to vertical deviation measured by the visual guidance system. The AUV remains hovering by using two vertical thrusters at 2 m.

(4) According to the transverse, longitudinal and heading angle deviations measured by the visual guidance system, the AUV's position relative to the recovery device is readjusted to control the deviation within an ideal range.

(5) The AUV continues to move slowly downward until it is 0.5 m away from the L-shaped light array of the recovery device. The AUV remains hovering by using two vertical thrusters at 0.5 m.

(6) The AUV moves towards the locking device by the main propeller, which captures and locks the docking rod, thus completing AUV recovery.

When the camera does not obtain most of the effective guidance information (the number of target light sources identified by the camera is less than three), the AUV recovery task is deemed as failure, and the AUV floats upward.

C. POSITIONING ALGORITHM

AUV in the state of no longitudinal inclination is AUV parallel to the L-shaped light array, in the actual recovery of AUV, the longitudinal inclination of AUV is less than 5° is considered to be AUV in the state of no longitudinal inclination.

The four-degree-of-freedom positioning of AUV can be determined according to any two light source targets. Take light A and light C as examples to calculate the vertical distance. The following formula (1) holds according to the principle of geometrical optics:

$$\frac{r_{ac}}{D_{ac}} = \frac{f}{H} \quad (1)$$

D_{ac} is the distance between light A and light C. Their corresponding image points are $I_A(x_1, y_1)$ and $I_C(x_2, y_2)$. The spacing between the two image points is r_{ac} . Δx , Δy are the projections of line segment $\overline{I_A I_C}$ on the X and Y axes respectively, $\Delta x = x_c - x_a$, $\Delta y = y_c - y_a$. $r_{ac} = \sqrt{\Delta x^2 + \Delta y^2}$, f is the focal length of the lens.

The distance between the camera and the L-shaped light array can be obtained:

$$H = \frac{D_{ac} \cdot f}{r_{ac}} = \frac{D_{ac} \cdot f}{\sqrt{\Delta x^2 + \Delta y^2}} \quad (2)$$

The length of docking rod l is 0.5 m, and the height of the locking device from the L-shaped light array ΔH is 0.5 m. Therefore, the vertical positioning distance can be calculated as follows:

$$H_{fin} = H - \Delta H - \frac{l}{2} \quad (3)$$

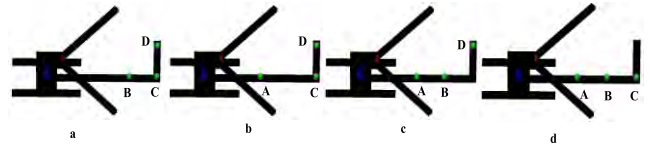


FIGURE 9. Four cases of partial target loss.

Take light B as an example to calculate relative lateral deviation and longitudinal deviation.

$$\begin{cases} x_b^c = \frac{H}{f} x_b \\ y_b^c = \frac{H}{f} y_b \end{cases} \quad (4)$$

The coordinates of the light B in camera coordinate system are (x_b^c, y_b^c, z_b^c) , the coordinates of the point of the light B in the image plane coordinate system are (x_b, y_b) . So, x_b^c is longitudinal deviation, y_b^c is lateral deviation, $z_b^c = H$.

(x_b^c, y_b^c, z_b^c) represent the relative position between the camera and the light B. The transformation matrix of the camera coordinate system to the AUV docking rod coordinate system is ${}^a X_c = (\Delta X^a + \Delta X_{bp}, 0, 0)^T$. So, the relative translation between the AUV docking rod and the L-shaped light array can be expressed as:

$$(x_b^a, y_b^a, z_b^a)^T = (x_b^c, y_b^c, z_b^c)^T + {}^a X_c \quad (5)$$

Take light A and light C as examples to calculate heading angle deviation. Suppose \overrightarrow{CA} is the forward direction of recovery device X^l , then the relative heading angle ψ is the angle between \overrightarrow{CA} and $\overrightarrow{OX^l}$. The relative heading angle $\psi \in (-\pi, \pi]$, the clockwise rotation direction is positive. Assuming that the coordinates of the image points of the light A and the light C in the image plane coordinate system are (x_a, y_a) and (x_c, y_c) , the relative heading angle calculation formula is as follows:

$$\psi = \begin{cases} -\arctan\left(\frac{y_c - y_a}{x_c - x_a}\right) & x_c > x_a \\ -\pi - \arctan\left(\frac{y_c - y_a}{x_c - x_a}\right) & x_c < x_a, y_c > y_a \\ \pi - \arctan\left(\frac{y_c - y_a}{x_c - x_a}\right) & x_c < x_a, y_c < y_a \end{cases} \quad (6)$$

The value of heading angle under special circumstances is as follows:

$$\psi = \begin{cases} \pi/2 & x_c = x_a, y_c < y_a \\ -\pi/2 & x_c = x_a, y_c > y_a \\ 0 & x_c > x_a, y_c = y_a \\ \pi & x_c < x_a, y_c = y_a \end{cases} \quad (7)$$

D. POSITIONING ALGORITHM FOR PARTIAL TARGET LOSS

AUV is constantly moving during the recycling process, ideally the camera can capture four target light sources, but in practice the camera may capture less than or equal to four target light sources. This article focuses on the situation shown in Figure 9.

When the lost target light is light D, that is, the L-shaped light array lost ‘-’ to ‘|’. According to ‘|’, the transverse, longitudinal, vertical deviation and the size of the heading angle deviation can be calculated. The heading angle direction takes the heading angle direction of the previous frame image; When the lost target light source is light A or light B, the overall shape of the light array is still ‘L’, which can first identify the overall shape and then calculate the posture information of four degrees of freedom; When the lost target light source is light C, the position of each light is determined by geometric relation, and then the posture information of four degrees of freedom is calculated. The key to the problem of partial loss of the target light source is to judge the lost target, identify the overall shape and relative position of the non-lost target, and then calculate the AUV posture information by using the positioning algorithm of 3.3 subsection.

The algorithm for identifying the relative position of the non-lost target light source is as follows:

(1) Set the centers of the three target light sources as X, Y, and Z in sequence. Take any two points to generate a straight line. That is, l_{XY}, l_{XZ}, l_{YZ} .

(2) Calculate the included angle Δ between any two straight lines.

1) If $\Delta \leq 5^\circ$, indicates that any two straight lines are substantially collinear. The three target light sources detected are arranged linearly, and the missing target light source is light D.

2) If $85^\circ \leq \Delta \leq 95^\circ$, indicates that there are two straight lines perpendicular, the lost target light source is light A or light B.

3) If $110^\circ \leq \Delta \leq 130^\circ$, indicates that there are two straight lines intersecting blunt angle, and the lost target light source is light C.

Since the probability of losing the target light source B is small, this situation will not be discussed. Even if the target light source B is lost, the L-shaped contour can be identified, so that the target light source which is not lost can be distinguished and posture information can be obtained. Selecting 3 images with partial target missing, and the simulation results are shown in Table 2.

E. IMPROVED JUDGMENT OF RELATIVE HEADING ANGLE

When the longitudinal inclination angle of AUV is greater than 5° , $\|BC\| \approx \|CD\|$, the above heading angle positioning algorithm will lead to wrong relative heading angle direction. The improved relative heading angle algorithm is as follows:


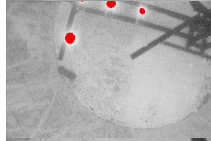
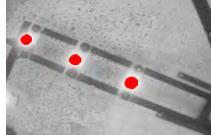
The pixel coordinates of the light A and the light C at the AUV longitudinal inclination θ are still (x_a^c, y_a^c) and (x_c^c, y_c^c) . Assuming that there is a pixel point E, its pixel coordinates are (x_e^c, y_e^c) , $x_e^c = x_c^c + \lambda, y_e^c = y_c^c, \lambda$ generally take 10.

The pixel spacing between light A and light C is:

$$r_{ac} = \sqrt{\Delta x^2 + \Delta y^2} \quad (8)$$

where $\Delta x = x_c - x_a, \Delta y = y_c - y_a$.

TABLE 2. The discrimination result of the target light source is not lost.

Simulation image	Target light source pixel position
	B [657.197, 136.941]
	C [513.205, 98.6845]
	D [456.691, 296.784]
	A [499.395, 34.9919]
	B [385.742, 10.3358]
	D [236.201, 128.933]
	A [68.5693, 171.407]
	B [233.164, 248.177]
	C [422.237, 335.653]

The pixel spacing between light C and E is:

$$r_{ce} = \sqrt{\Delta x_0^2 + \Delta y_0^2} \quad (9)$$

where $\Delta x_0 = x_c - x_e, \Delta y_0 = y_c - y_e$.

The heading angle of AUV relative to L-shaped light array is:

$$\psi = \begin{cases} \arccos \theta & \cos \theta > 0, \tan \theta > 0 \\ -\arccos \theta & \cos \theta > 0, \tan \theta < 0 \\ -\arccos \theta & \cos \theta < 0, \tan \theta > 0 \\ \arccos \theta & \cos \theta < 0, \tan \theta < 0 \end{cases} \quad (10)$$

where $\cos \theta = \frac{\Delta x \cdot \Delta x_0 + \Delta y \cdot \Delta y_0}{r_{ac} \cdot r_{ce}}, \tan \theta = -\frac{\Delta y}{\Delta x}$.

The captured underwater images are simulated to obtain the simulation results as shown in Figure 10. Figure 10(a) shows that the discrimination result of the unimproved relative heading angle is 179° , Figure 10(b) shows that the judgment result of the improved relative heading angle is -1° . When the actual course of AUV is 0° , under the influence of longitudinal inclination, the non-improved relative heading angle discriminating algorithm will get the result of AUV heading 180° . AUV will receive the steering command and gradually deviate from the expected course. The course judged by the improved method is the true course of AUV 0° , which ensures that the acquisition of information is true and effective, so that AUV can reach the desired position under autonomous control.

IV. EXPERIMENTS AND RESULTS

A. HARDWARE COMPOSITION

The test AUV is a hover-capable AUV. The AUV has a rear propeller, four control surfaces, and two vertical and two horizontal tunnel thrusters as Figure 11, related details are shown in Table 3. The AUV’s depth and pitch are controlled by the two vertical tunnel thrusters at low velocities, while the AUV’s yaw and sway are controlled by the two horizontal tunnel thrusters. The AUV could control five degrees-of-freedom (DOF) at low speeds, but when operating at high

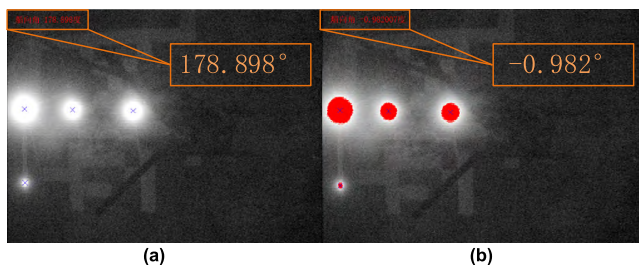


FIGURE 10. Non-improved algorithm (a) and improved algorithm (b).

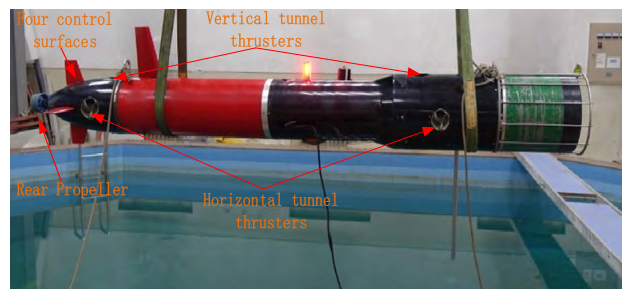


FIGURE 11. The test AUV.

TABLE 3. Related AUV details.

Item	Specification
Number of actuators	9
Weight in air	120 kg
Speed	Maximum speed: 5 kn Economical speed: 2 kn
Overall length	2.8 m
Diameter	256 mm
Depth rating	100 m
Control period	0.5 s
Endurance	8 hrs
Energy source	Lithium ion battery

TABLE 4. Hardware parameter information of visual guidance system.

Item	Specification	Quantity
LED target light source	Operating depth: 150 m,	4
	Luminous flux: 970 lm /367 lm,	
	Effective range: 253 m	
Underwater camera	Effective pixels: 768×576, Minimum illumination: 0.02Lux,	1
	Focal length: 3.8 mm, Voltage: 24VDC Angle of view: 68.5°	
Image acquisition card	Bus mode: PCI04-PLUS, Video input mode: One-way composite video input,	1
	Maximum resolution of image PAL standard: 768×576×24 bit	
Guidance computer	Processor: Intel Pentium M,	1
	Frequency: 1.4 GHz, Memory: 512 M	

speeds the AUV could control six DOF. The AUV is over-actuated when operating at high speeds, with more active actuators than DOF.

The visual guidance system consists of four parts: LED target light source, underwater camera, image acquisition card, guidance computer. As shown in Figure 12, the specific parameters of each part are shown in Table 4.

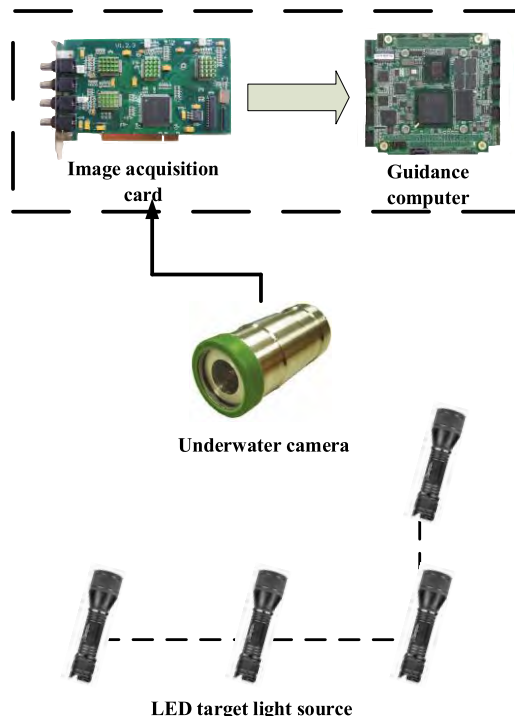


FIGURE 12. Composition of visual guidance system.

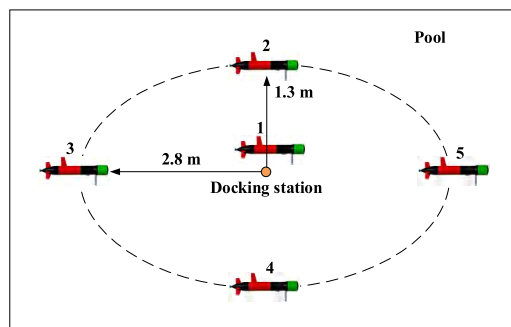


FIGURE 13. The AUV departs from different position.

B. AUV RECOVERY AND DOCKING EXPERIMENT

Before the docking recovery test, the AUV camera needs calibrating. And the positioning deviation of the visual guidance system in transverse, longitudinal and vertical direction needs testing. A hanging rod is installed on the sliding table beside the pool, the other end of the hanging rod is fixed with a camera and submerged, moving the sliding table simulates the actual loading effect of the AUV. The recovery device is fixed at a known position in the pool, and the sliding table drives the camera to move. The positioning deviation of the visual guidance system can be obtained by comparing the camera positioning information with the position information given by the sliding table. After testing, the transverse positioning deviation of the visual guidance system is less than or equal to 0.2 m, the longitudinal positioning deviation is less than or equal to 0.15 m, and the vertical positioning deviation is less than or equal to 0.15 m, which satisfies the requirements of Fork column recovery test.

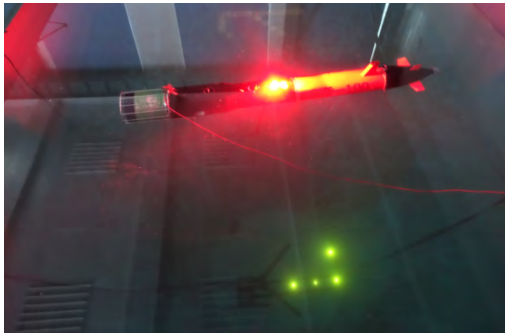


FIGURE 14. AUV recovery test.

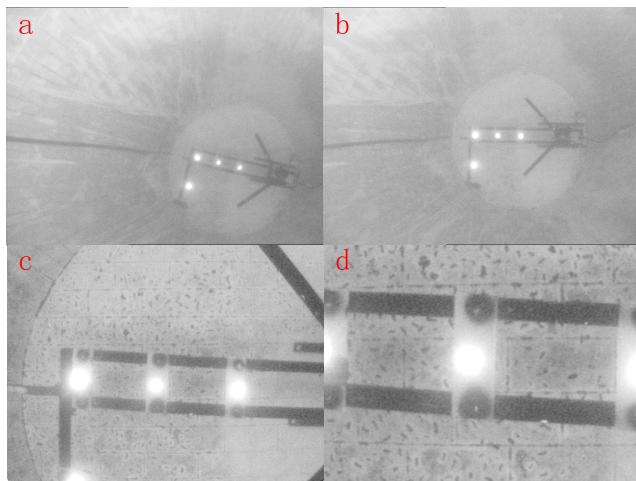


FIGURE 15. AUV docking course.

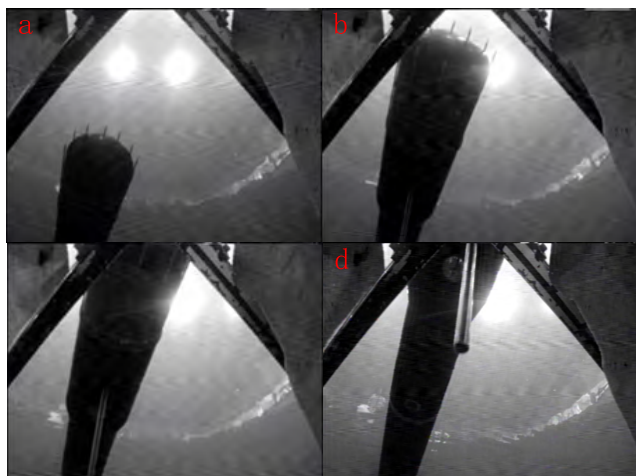


FIGURE 16. AUV successful docking.

The fork-carrying-pole recovery test was carried out in the laboratory pool in 2018, and its dimension is $10\text{ m} \times 5\text{ m} \times 5\text{ m}$. Considering that the visual field of the camera in water is limited to 68.5° and the AUV is easy to collide when adjusting the heading angle. Therefore, a virtual ellipse with a major axis radius of 2.8 m and a minor axis radius of 1.3 m is made with the docking station as the origin. The range of virtual ellipses is the effective recycling range. The draft is shown as Figure 13. Four points on the virtual

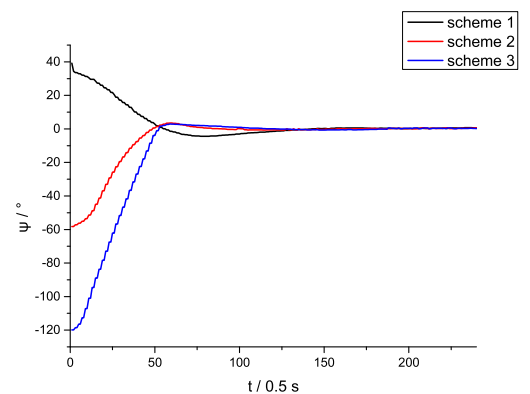
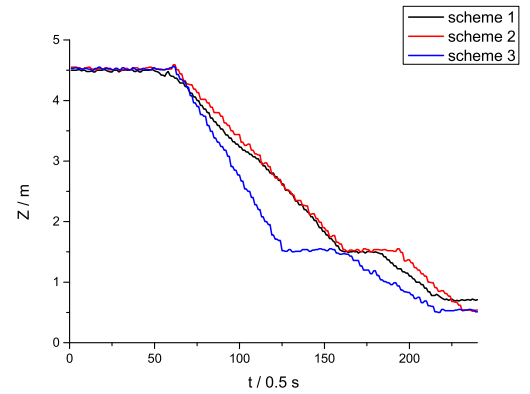
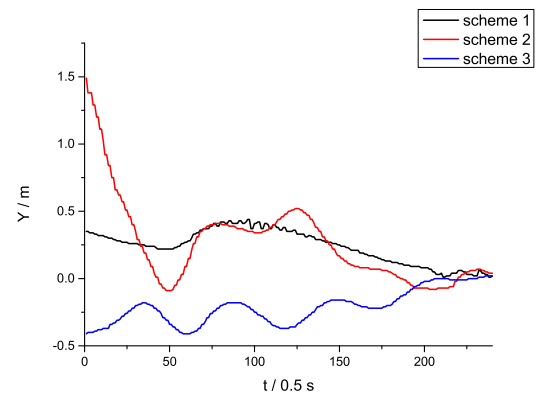
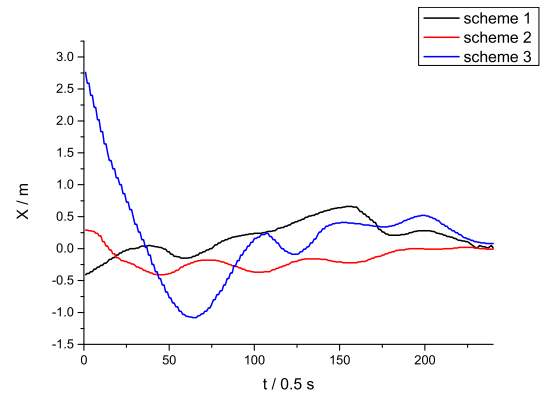


FIGURE 17. Deviation of the vision guidance system of X, Y, Z, ψ .

ellipse boundary and the point above the docking station are selected as starting points for the experiment. The AUV is placed at these five different positions with different heading

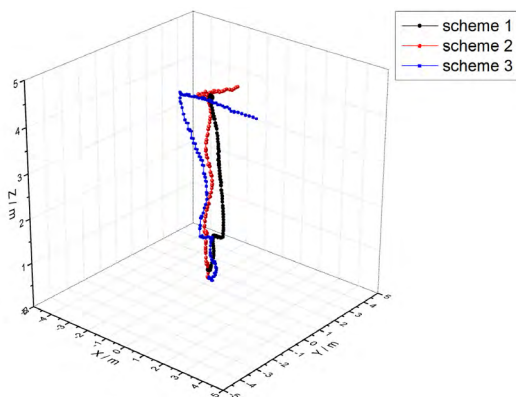


FIGURE 18. The spatial trajectories of the AUV relative to the recovery device.

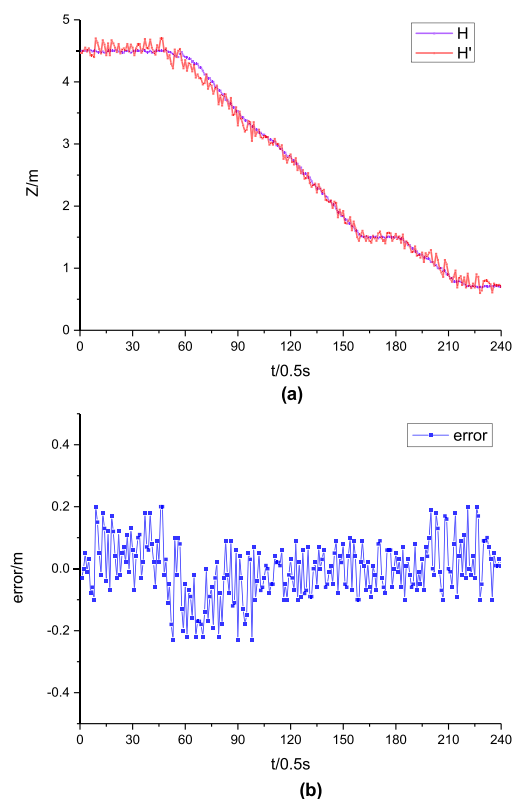


FIGURE 19. Vertical relative distance given by visual guidance and depth gauge (a) and vertical relative distance error given by visual guidance and depth gauge (b).

angle. And five schemes are designed. In this part, scheme 1 is introduced. Since point 2 and point 4, point 3 and point 5 are symmetrical about the origin, only the experimental data of scheme 2 and scheme 3 are given to prove the validity of the test.

Using two slings places the recovery device at the bottom of the pool and adjusts the angle. After everything is ready, placing the AUV at 4.5 m above the recovery device makes it at any angle with the recovery device shown in the Figure 14.

Send the recovery command to AUV and start the recovery task. Figure 15 shows the docking course taken by the AUV camera during the movement. The AUV adjusts its heading

and moves downward gradually. The posture of AUV is adjusted at 1.5 m and 0.5 m away from the L-shaped light array of the recovery device respectively. The AUV keeps the posture and prepares docking with the recovery device. As shown in the Figure 16, the AUV moves towards locking device and successfully docks with the recovery device taken by the camera mounted under V-shaped shears. These pictures verify the feasibility of the fork-carrying-pole recovery docking device and the stability of the visual positioning method.

Figure 17 shows the deviation of the vision guidance system in the four degrees of freedoms during the AUV movement. Figure 18 shows the spatial trajectory of the AUV relative to light B.

Due to the poor guidance effect of the USBL guidance system in the small pool, the complete comparison of the three-dimensional position of AUV cannot be given. The coordinates of the AUV in the vertical plane can be given simultaneously by the visual guidance system and the pressure depth gauge. The relationship between the two is as a formula:

$$H' = H_L - D - d \tag{11}$$

$H_L = 4.5\text{ m}$ is the distance between the L-shaped light array and the water surface, D is AUV real-time depth given for pressure depth gauge, d is the distance between the pressure depth gauge and the camera plane in the vertical direction. H' is the distance between the camera and the L-shaped light array derived from the pressure depth gauge. Under ideal circumstances $H' = H_{fm}$. Here, the comparison between the two is given by taking scheme 1 as an example shown in Figure 19, it can be seen from the figure that the vertical distance given by the visual guidance system is more stable than that given by the pressure depth gauge, and the deviation between the two is less than or equal to 0.2 m. Other schemes are also analyzed, and the conclusions are the same as before.

V. CONCLUSION

This paper introduces the fork-carrying-pole recovery docking device and the L-shaped light array. The four-degree-of-freedom positioning algorithm and the target light source discrimination algorithm for the L-shaped light array are proposed. The positioning method in the case of partial target light source loss is solved. In view of the fact that the AUV has a longitudinal inclination angle (heeling angle), the heading angle judgment is improved to enhance the AUV’s heading control capability. The method of the fork-carrying-pole recovery is verified by the pool experiment. The vertical positioning deviation of visual guidance is less than 0.2 m. The experiment proves that the system can realize recovery of AUV, and verifies the feasibility of L-shaped light array and the stability of visual guidance. In the complex underwater environment, the proposed four-degree-of-freedom positioning method is not ideal for positioning where there is a large longitudinal inclination angle, only the relative heading

angle deviation can be judged, which will be the focus of improvement in future work.

VI. ACKNOWLEDGMENTS

The authors would like to thank everyone involved for their contributions to this article.

REFERENCES

- [1] W. Zhang, Y. Teng, S. Wei, H. Xiong, and H. Ren, "The robust H-infinity control of UUV with Riccati equation solution interpolation," *Ocean Eng.*, vol. 156, pp. 252–262, May 2018.
- [2] X. Sheng, Y. Liu, H. Liang, F. Li, and Y. Man, "Robust visual tracking via an improved background aware correlation filter," *IEEE Access*, vol. 7, pp. 24877–24888, 2019.
- [3] Z. Yan, H. Yu, W. Zhang, B. Li, and J. Zhou, "Globally finite-time stable tracking control of underactuated UUVs," *Ocean Eng.*, vol. 107, pp. 132–146, Oct. 2015.
- [4] W. Zhang, T. Yanbin, W. Shilin, S. Hu, and J. Zhang, "Underactuated UUV tracking control of adaptive RBF neural network and backstepping method," *J. Harbin Eng. Univ.*, vol. 39, no. 1, pp. 93–99, Jan. 2018.
- [5] S. Liu, M. Ozay, T. Okatani, H. Xu, K. Sun, and Y. Lin, "Detection and pose estimation for short-range vision-based underwater docking," *IEEE Access*, vol. 7, pp. 2720–2749, 2019.
- [6] W. Zhang, S. Wei, Y. Teng, J. Zhang, X. Wang, and Z. Yan, "Dynamic obstacle avoidance for unmanned underwater vehicles based on an improved velocity obstacle method," *Sensors*, vol. 17, no. 12, p. 2742, Nov. 2017.
- [7] H. Singh, J. G. Bellingham, F. Hover, S. Lemer, B. A. Moran, K. von der Heydt, and D. Yoerger, "Docking for an autonomous ocean sampling network," *IEEE J. Ocean. Eng.*, vol. 26, no. 4, pp. 498–514, Oct. 2001.
- [8] M. Wirtz, M. Hildebrandt, and C. Gaudig, "Design and test of a robust docking system for hovering AUVs," in *Proc. OCEANS*, Hampton Roads, VA, USA, Oct. 2012, pp. 1–6.
- [9] D. Li, Y.-H. Chen, J.-G. Shi, and C.-Y. Yang, "Autonomous underwater vehicle docking system for cabled ocean observatory network," *Ocean Eng.*, vol. 109, pp. 127–134, Nov. 2015.
- [10] K. Teo, B. Goh, and O. K. Chai, "Fuzzy docking guidance using augmented navigation system on an AUV," *IEEE J. Ocean. Eng.*, vol. 40, no. 2, pp. 349–361, Apr. 2015.
- [11] L. Wu, Y. Li, S. Su, P. Yan, and Y. Qin, "Hydrodynamic analysis of AUV underwater docking with a cone-shaped dock under ocean currents," *Ocean Eng.*, vol. 85, pp. 110–126, Jul. 2014.
- [12] Y. Li, Y. Jiang, J. Cao, B. Wang, and Y. Li, "AUV docking experiments based on vision positioning using two cameras," *Ocean Eng.*, vol. 110, pp. 163–173, Dec. 2015.
- [13] K. Teo, E. An, and P.-P. J. Beaujean, "A robust fuzzy autonomous underwater vehicle (AUV) docking approach for unknown current disturbances," *IEEE J. Ocean. Eng.*, vol. 37, no. 2, pp. 143–155, Apr. 2012.
- [14] A. Hartmann, M. Kralik, F. Humer, J. Lange, and M. Weiler, "Identification of a karst system's intrinsic hydrodynamic parameters: Upscaling from single springs to the whole aquifer," *Environ. Earth Sci.*, vol. 65, no. 8, pp. 2377–2389, Apr. 2012.
- [15] Q. Liu, G. Hu, and M. M. Islam, "Robust visual tracking with spatial regularization kernelized correlation filter constrained by a learning spatial reliability map," *IEEE Access*, vol. 7, pp. 27339–27351, 2019.
- [16] W. Huang, J. Gu, X. Ma, and Y. Li, "Correlation-filter based scale-adaptive visual tracking with hybrid-scheme sample learning," *IEEE Access*, vol. 6, pp. 125–137, 2017.
- [17] Y. Fang, Y. Yuan, L. Li, J. Wu, W. Lin, and Z. Li, "Performance evaluation of visual tracking algorithms on video sequences with quality degradation," *IEEE Access*, vol. 5, pp. 2430–2441, 2017.
- [18] A. Negre, C. Pradalier, and M. Dunbabin, "Robust vision-based underwater target identification and homing using self-similar landmarks," in *Proc. 6th Int. Conf. Field Service Robot.*, Chamonix, France, 2007, pp. 51–60.
- [19] J.-P. Park, B.-H. Jun, P.-M. Lee, and J. Oh, "Experiments on vision guided docking of an autonomous underwater vehicle using one camera," *Ocean Eng.*, vol. 36, no. 1, pp. 48–61, Jan. 2009.
- [20] J. Zhou, W. Zhang, D. Wu, and Y. Hao, "Underwater recovery realization for an AUV using positioning-to-line strategy," in *Proc. ITEC Asia-Pacific*, Beijing, China, Aug./Sep. 2014, pp. 1–5.
- [21] S. Ghosh, R. Ray, S. R. K. Vadali, S. N. Shome, and S. Nandy, "Reliable pose estimation of underwater dock using single camera: A scene invariant approach," *Mach. Vis. Appl.*, vol. 27, no. 2, pp. 221–236, Feb. 2016.

• • •